

Design of Electromagnetic modes in photonic crystal optical waveguides

Sasank Reddy and Ali Adibi

School of Electrical and Computer Engineering
Georgia Institute of Technology, Atlanta, GA 30332-0250
e-mail: gte326n@prism.gatech.edu, adibi@ee.gatech.edu

Yong Xu and Reginald K. Lee

Orbits Lightwave Inc.
101 Waverly Dr., Pasadena, CA 91105
e-mail: yong@its.caltech.edu, leereg@caltech.edu

ABSTRACT

We present a systematic method for designing electromagnetic modes in dielectric-core photonic crystal optical waveguides. We show that the guided modes of the photonic crystal waveguides are mainly confined to the guiding region. The properties of these modes can be modified by changing the geometry of the air holes next to the guiding region. We show how this concept can be used to design single-mode photonic crystal waveguides. We also describe a method for changing the slope of the dispersion diagrams of these guided modes.

Keywords: Photonic crystals, Photonic bandgap, Planar waveguides, Photonic crystal waveguides, Distributed Bragg reflection

1. INTRODUCTION

Photonic crystals^{1,2} have inspired a lot of interest recently due to their potential for controlling the propagation of light. Photonic crystals with line defects can be used for guiding light. Waveguides using one-dimensional periodic structures were proposed by Yeh et al.³ Guiding light through sharp bends has been recently proposed⁴ and demonstrated at microwave⁵ and optical^{6,7} frequencies. Several aspects of the photonic crystal waveguides have been investigated.⁸⁻¹⁵ In all the proposals and demonstrations of photonic bandgap (PBG) waveguides, the guiding modes were restricted to the photonic bandgap of the infinite photonic crystal. Furthermore, the PBG waveguides in the previous reports⁴⁻⁶ were made by removing one row of either air columns or dielectric rods that results in multimode guiding. Single mode waveguides, however, are more desirable for practical applications. We recently studied¹⁶ a more general type of PBG waveguide which consists of a dielectric slab placed between two PBG mirrors. Such a PBG waveguide can be made single mode by choosing the appropriate thickness for the dielectric slab.^{16,17} However, the centers of the air holes above and below the middle slab are not located on the same lattice due to the arbitrary slab thickness. This makes the design of waveguide bends complicated. The centers of the air holes in a single-mode waveguide for practical applications (like all-optical circuits) must be on the same lattice.

One major advantage of photonic crystals is the possibility of designing electromagnetic modes. The ability to modify the dispersion diagram of a guided mode in a photonic crystal waveguide is very useful for practical applications. In this paper, we present an idea for designing electromagnetic modes in photonic crystal waveguides. We show that the dispersion diagrams of the guided modes of a PBG waveguide can be considerably modified by changing the geometry of the air holes adjacent to the middle slab. In section 2 we summarize the simulation method we use in this paper. The guiding mechanisms in a PBG waveguide are discussed in Section 3. In Section 4 we discuss the design of single-mode photonic crystal waveguides without breaking the periodicity of the centers of the air holes in a two-dimensional photonic crystal. In section 5 we present an idea for modifying the slope of the dispersion diagram of the guided modes of a PBG waveguide. Conclusions are made in Section 6.

2. SIMULATIONS

The main structure we use in the analysis of this paper is the photonic crystal waveguide made by adding a line defect to a perfect two-dimensional photonic crystal. The photonic crystal we use throughout this paper is a two-dimensional lattice of infinite air columns in gallium arsenide (GaAs) as shown in Figure 1. To analyze the guiding structures, we use a computer code based on the two-dimensional finite difference time domain (2D-FDTD) method.¹⁸ To calculate the dispersion diagram of the guided modes of a PBG waveguide, we use an order- N spectral method¹⁹ in the computational domain. The computational domain is made of one period of the guiding structure in the guiding direction, and it is thick enough in the perpendicular to direction to assure the guided modes do not feel the artificial boundary (for an example of a computational domain, see Figure 1 (a)) We use Bloch boundary conditions on the left and right sides and perfectly matched layers (PML)²⁰ on the top and bottom of the guiding structure (see Figure 1 (a)). The electric or magnetic field patterns of the guided modes of the PBG waveguide at different frequencies were obtained through a similar procedure by exciting the structure with a constant frequency source. More details of our numerical algorithms can be found in our previous publications.^{21,22} In the calculations of this paper, the speed of light in vacuum (c) is normalized to 1, and all spatial dimensions are in the units of calculation cells.

3. GUIDING MECHANISMS IN A PBG WAVEGUIDE

Two important physical mechanisms for guiding light in PBG waveguides are total internal reflection (due to the index contrast between middle slab and cladding) and Bragg reflection (due to the presence of photonic crystal). In this section, we discuss the importance of each mechanism for a typical PBG waveguide.

Figure 1 (a) shows one unit cell of a PBG waveguide made by placing a dielectric slab of thickness d between two PBG mirrors, each consisting of a two-dimensional square lattice of air columns in GaAs. The period of the square lattice and the radius of each air column are a and $r = 0.45a$, respectively. In the simulations of this section, we choose $a = 24$ calculation cells. The waveguide shown in Figure 1 (a) is a single-mode waveguide in the photonic bandgap as discussed previously.¹⁶ Since GaAs has a large index of refraction ($\epsilon_{\text{GaAs}} \simeq 13$ at $\lambda = 1.55$ nm), total internal reflection (TIR) at the boundary of the middle slab and the PBG cladding can result in the confinement and guiding of optical energy in the middle slab. To investigate the strength of TIR, we can compare the dispersion diagram of the guided mode of the PBG waveguide with that of a conventional dielectric slab waveguide shown in Figure 1 (b). The permittivity and the thickness of the slab waveguide in Figure 1 (b) are the same as those of the middle slab of the PBG waveguide (ϵ_{GaAs} and d , respectively). One difference between the PBG waveguide and the slab waveguide shown in Figure 1 is the periodic corrugation in the PBG waveguide. Since the guided mode of the PBG waveguide is mainly confined in the middle slab, an important role is played by the two rows of the air columns that are adjacent to (one on each side of) the middle slab. Due to the periodicity of these air columns, the guided mode is affected by distributed Bragg reflection (DBR). To observe the effect of the DBR on the guided mode, we compare the dispersion diagram of the guided mode of the PBG waveguide with that of the equivalent corrugated waveguide shown in Figure 1 (c). The equivalent corrugated waveguide is made by reducing the thickness of each PBG mirror in Figure 1 (a) to r . This results in a one-dimensional periodic waveguide with period a .

Figure 1 (d) shows the dispersion diagrams for the fundamental TE modes (electric field normal to the computation plane) of the three waveguides shown in Figures 1 (a), (b), and (c). The dispersion diagram of the slab waveguide mode in Figure 1 (b) is restricted to the first Brillouin zone of the slab waveguide with imposed artificial spatial periodicity the same as that of the PBG waveguide. The photonic bandgap (PBG) of the two-dimensional photonic crystal of Figure 1 (a) is also shown in Figure 1 (d). The similarity between the fundamental modes of the PBG and the slab waveguides proves that total internal reflection plays a major role in PBG waveguides. The fundamental modes of the two waveguides will be more similar²³ if we replace air in the cladding of the slab waveguide in Figure 1 (b) with a material with permittivity (ϵ_{ave}) equal to the average permittivity of the PBG mirrors ($\epsilon_{\text{ave}} = [\epsilon_{\text{air}} \times \pi r^2 + \epsilon_{\text{GaAs}} \times (a^2 - \pi r^2)]/a^2$). The difference between the fundamental modes of the PBG waveguide and the slab waveguide is due to distributed Bragg reflection in the former. As Figure 1 (d) shows, the dispersion diagram of the fundamental mode of the PBG waveguide is approximately the same as that of the fundamental mode of the equivalent corrugated waveguide, which incorporates the effects of both TIR and DBR. This suggests that the combination of TIR and DBR is responsible for the properties of the fundamental guided mode in the PBG waveguide. Figure 1 (d) also suggests that the properties of the fundamental guided mode of the PBG waveguide are mainly controlled by the two rows, one on each side, of the photonic crystal that are adjacent to the middle slab. Therefore, we can replace a PBG waveguide by its equivalent corrugated waveguide to obtain the approximate behavior. Such

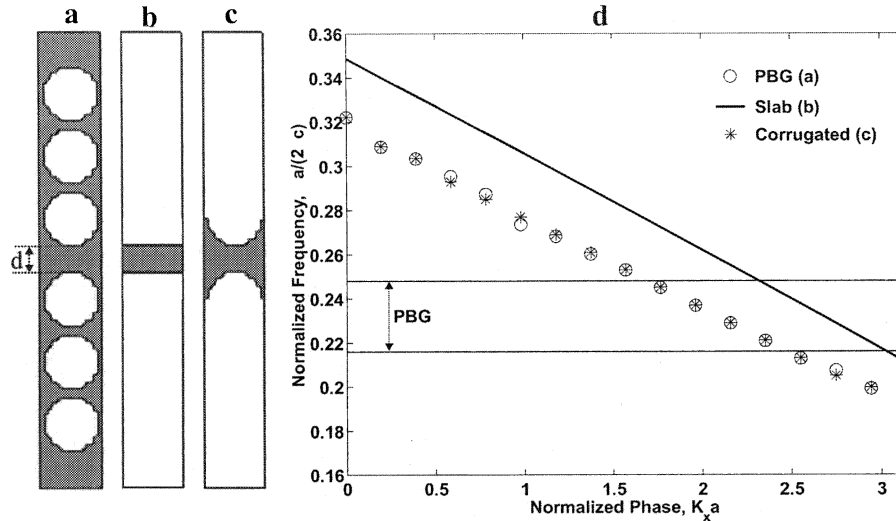


Figure 1. Guiding mechanisms in a PBG waveguide: one period of (a) a PBG waveguide, (b) the corresponding dielectric slab waveguide, and (c) the corresponding corrugated waveguide. The thickness of the middle slab in all three waveguides is $d = 9$ calculation cells. The period and the radius of the air holes in the PBG waveguide are $a = 24$ calculation cells and $r = 0.45a$, respectively. The dielectric used in this paper is GaAs ($\epsilon = 12.96$). (d) Dispersion diagram of the fundamental TE (electric field normal to the computation plane) modes of the waveguides in parts (a), (b), and (c).

a replacement is also useful in obtaining approximate analytic formulas for the properties of the fundamental guided mode of a PBG waveguide, since the analysis of corrugated waveguides is straightforward.²⁴

The main difference between the PBG waveguide and the corrugated waveguide is that the guiding frequencies in the former is limited by the modes of the photonic crystal. Guiding in a PBG waveguide occurs only at frequencies where there is no interaction between the waveguide mode and the extended modes of the photonic crystal cladding. Such interactions can occur only outside the complete photonic bandgap (PBG) since the photonic crystal has no modes inside the PBG. The actual frequency range over which the waveguide mode has no interaction with the photonic crystal modes is usually larger than the complete PBG.¹⁷ It is defined by the bandgap of the photonic crystal in the guiding direction. Note that as long as the guided modes of the PBG waveguide are concerned, the PBG waveguide can be replaced by the equivalent corrugated waveguide.

We showed here that the properties of the guided modes of the PBG waveguide are mainly controlled by the two rows of the photonic crystal that are adjacent to the middle slab. In the next two sections of this paper, we concentrate on the modification of the dispersion diagrams of the guided modes of a PBG waveguide by changing the properties of these two rows.

4. DESIGN OF SINGLE-MODE PBG WAVEGUIDES WITH CONSERVED PERIODICITY OF THE AIR HOLES

PBG waveguides with single-mode propagation in the photonic bandgap are essential parts of any photonic crystal circuit. The PBG waveguide shown in Figure 1 (a) has only one guided mode in the photonic bandgap due to its thin slab. The major disadvantage of this PBG waveguide is the imposed downward vertical shift of the centers of the air holes above the middle slab. As a result, the centers of the air holes above the slab and those of the air holes below the slab are not on the same two-dimensional lattice. In other words, the distance between the center of an air hole above the slab and that of an air hole below the slab is not a multiple of period (a). This makes the design of waveguide bends complicated, especially when multiple cascaded bends must be designed. This is why the conventional PBG waveguides are made by removing one row of air holes. These conventional waveguides have multiple guided modes (at least two modes) due to their thick slab. Figure 2 (a) shows one period of a conventional

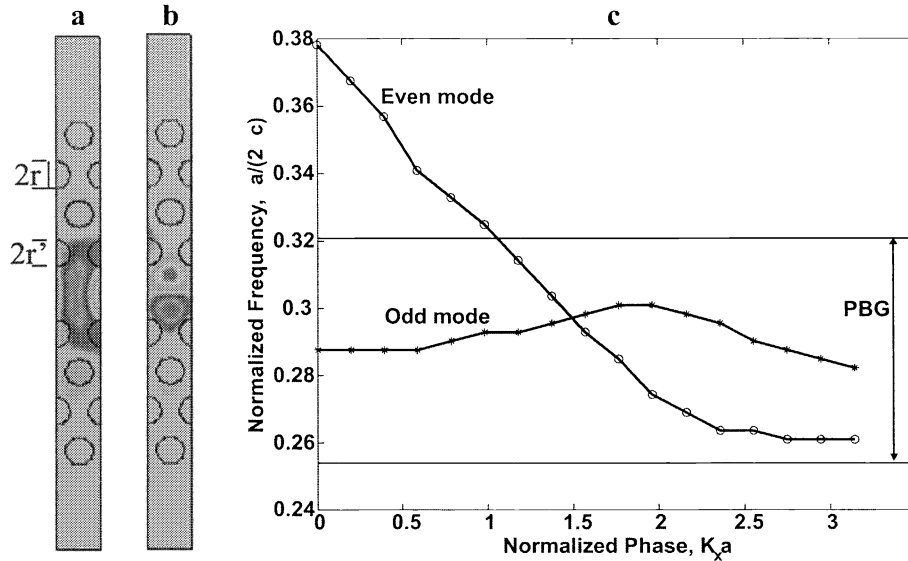


Figure 2. Magnetic field patterns for the (a) even and (b) odd TM (magnetic field normal to the computation plane) modes of a conventional PBG waveguide made by removing one row of air holes from a triangular lattice. (c) Dispersion diagrams of the two guided TM modes in the PBG waveguide shown in parts (a) and (b). The period and the radius of the air holes in the PBG waveguide are $a = 24$ calculation cells and $r = r' = 0.30a$, respectively.

PBG waveguide made by removing one row of air holes from a triangular lattice. The ratio between the radius of an air column (r) and the lattice period in the horizontal direction (a) is $r/a = 0.3$. In the simulations of this section, we choose $a = 24$ calculation cells. Figure 2 (c) shows the dispersion diagrams of the TM modes (magnetic field perpendicular to the computation plane) of the PBG waveguide. The PBG waveguide has two guided modes, one with even symmetry and the other one with odd symmetry. The magnetic field patterns of the two modes are shown in Figures 2 (a) and (b). In order to obtain single-mode propagation within the PBG, we need to reduce the thickness of the middle slab of the PBG waveguide.

One idea to reduce the effective thickness of the middle slab of the conventional PBG waveguide is to increase the radii of the air holes that are adjacent to the middle slab.²⁵ The centers of these air holes in this design are not modified. Figures 3 (a) and (b) show the dispersion diagrams of the even and odd modes, respectively, for different radii of the air columns in the two rows adjacent to the middle slab (r'). The radii of all other air columns are $r = 0.30a$ in all cases. Figure 3 (b) shows that for $r'/a > 0.40$ the odd mode is pushed out of the photonic bandgap, while the even mode still covers a considerable portion of the bandgap (except for $r'/a \simeq 0.50$). Therefore, we can obtain single-mode guiding in the PBG by choosing $r'/a > 0.40$. However, choosing r too large results in the excessive upward shift of the even mode reducing the frequency range for single-mode propagation in the PBG. Therefore, the optimum value of r'/a is about 0.40. Figure 4 shows the patterns of the magnetic field of the odd TM mode at $K_x a = 3\pi/4$ for different values of r'/a . The field patterns at $r'/a = 0.45$ and $r'/a = 0.50$ (Figures 4 (c) and (d), respectively) show that the odd mode is out of the PBG at these values of r'/a , since the field is extended to the surrounding photonic crystal regions. This is in agreement with the dispersion diagrams of the odd mode at these values of r'/a shown in Figure 3 (b). The low loss of the optical mode of the waveguide with $r'/a = 0.40$ (even though the mode frequency $\omega a/(2\pi c) = 0.330$ is slightly out of the bandgap) is due to the absence of the photonic crystal modes at that frequency and at the given phase constant ($K_x a = 3\pi/4$). Note that $0.254 < \omega a/(2\pi c) < 0.321$ represents the absolute (or complete) bandgap of the photonic crystal. The bandgap (frequency range with no mode present) at a specific value of $K_x a$ can be wider than the absolute bandgap.

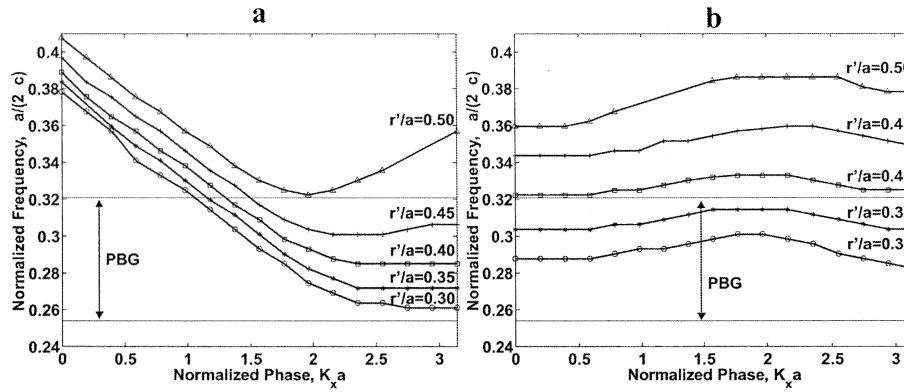


Figure 3. Dispersion diagrams for the (a) even and (b) odd TM modes, respectively, of the PBG waveguide in Figure 2 (a) for different radii of the air holes adjacent to the middle slab (r'). The radius of all other air holes is $r = 0.3a$.

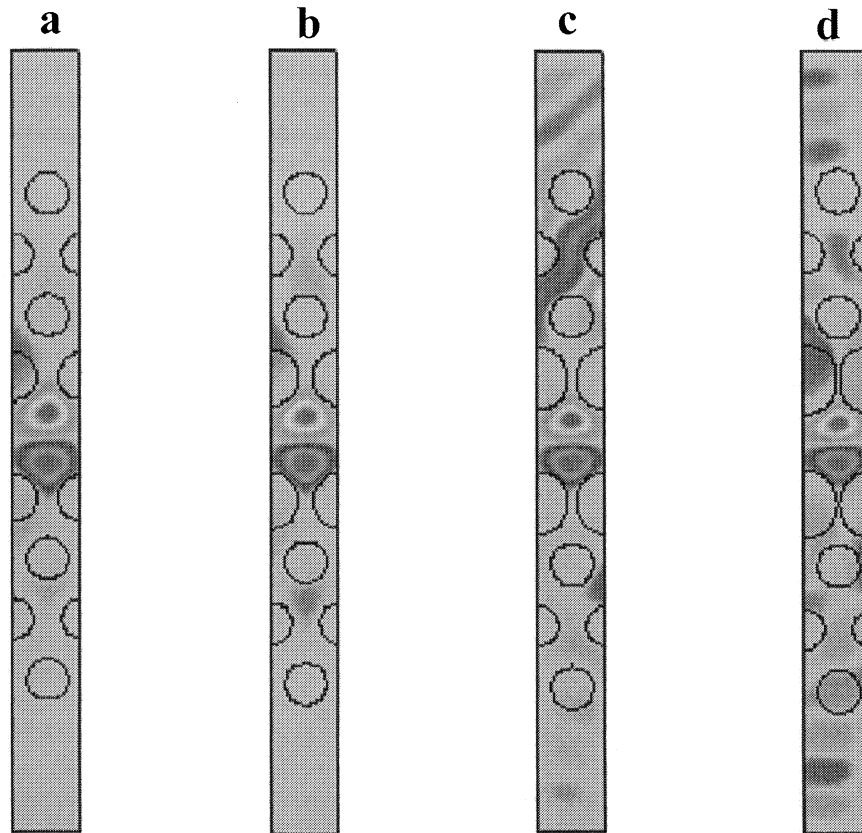


Figure 4. Magnetic field (B) patterns of the odd TM mode of the PBG waveguide shown in Figure 2 (a) at normalized phase ($K_x a = 3\pi/4$) with (a) $r' = 0.35a$ and $\omega a/(2\pi c) = 0.311$, (b) $r' = 0.40a$ and $\omega a/(2\pi c) = 0.330$, (c) $r' = 0.45a$ and $\omega a/(2\pi c) = 0.359$, and (d) $r' = 0.50a$ and $\omega a/(2\pi c) = 0.416$. In all four cases, $r = 0.30a$. The photonic bandgap is $0.254 < \omega a/(2\pi c) < 0.321$.

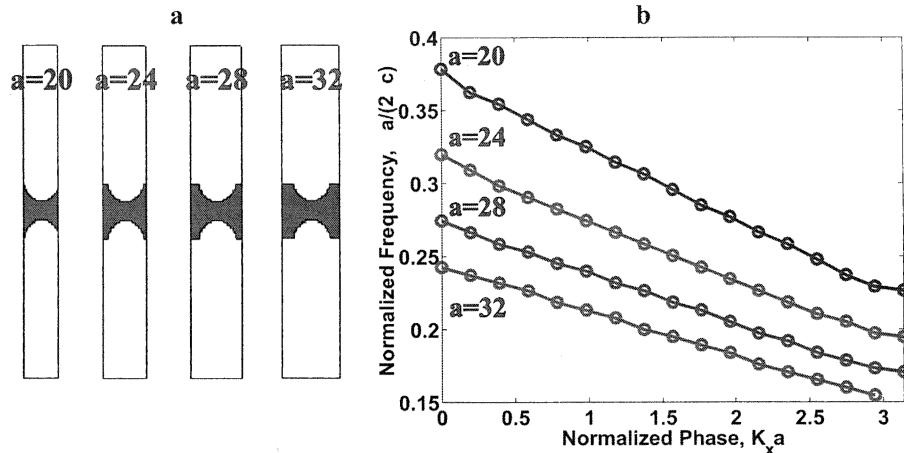


Figure 5. (a) Corrugated waveguides with similar corrugation and different periods (a). The shapes of all corrugations are half-circles with radius $r = 11$ calculations cells. (b) Dispersion diagrams for the fundamental TE modes of the corrugated waveguides shown in (a).

5. MODIFYING THE DISPERSION DIAGRAM OF THE GUIDED MODES IN A PBG WAVEGUIDE

In Section 4, we moved the dispersion diagrams of the guided modes of a PBG waveguide to different frequencies by changing the sizes of the air holes adjacent to the middle slab. In this section, we present a simple idea for changing the slope of the dispersion diagram of the guided modes by changing the periodicity of the air holes adjacent to the middle slab. For simplicity of the analysis, we use the equivalent corrugated waveguide for our simulations.

Figure 5 (a) shows several equivalent corrugated waveguides for a PBG waveguide as described in Section 3. The radius of the air holes in all these waveguides is the same, but the period of these air holes in the guiding direction is different for different waveguides. The dispersion diagrams of the corrugated waveguides with different periods are shown in Figure 5 (b). Some change in the slope of the dispersion diagram by changing the period (a) can be seen from Figure 5 (b). However, this change is overshadowed by the large frequency shift of the dispersion diagrams caused by changing the period as well. This frequency shift is due to the larger effective slab thickness for larger periods. Note that a corrugated waveguide with larger a is composed of larger dielectric regions compared to a waveguide with smaller a . Therefore, by increasing a , we effectively increase the slab thickness and move the mode dispersion diagrams to lower frequencies. To reduce this unwanted frequency shift, we can increase the radius of the air holes of the structures with larger a to keep the effective thickness of the middle slab constant. The corrugated waveguides made by this idea are shown in Figure 6 (a). The dispersion diagrams for the fundamental guided mode of these waveguides are shown in Figure 6 (b). Figure 6 (b) shows the reduction in the unwanted frequency shift by modifying the properties of the air holes adjacent to the middle slab. It also shows the change in the slope of the dispersion diagram of the fundamental guided mode caused by the appropriate modification of the size and period of the holes adjacent to the middle slab.

The results shown in this section suggest that there is a clear potential for the complete design of electromagnetic modes in a photonic crystal optical waveguide by modifying the geometry and periodicity of the air holes adjacent to the middle slab. We regard this powerful ability as a unique property of photonic crystals for the design of novel optical devices.

6. CONCLUSIONS

We presented here a systematic method for modifying the dispersion diagrams of the guided modes in a dielectric-core PBG waveguide. We showed that the properties of these guided modes are controlled by total internal reflection (TIR) and distributed Bragg reflection (DBR) from the periodic structure in the guiding direction. These guided

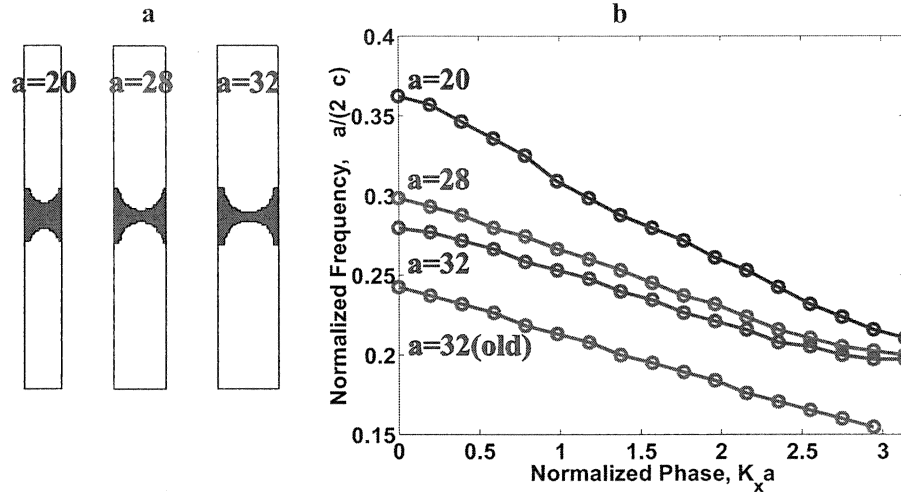


Figure 6. (a) Corrugated waveguides with different corrugation and different periods. The radius of the circular corrugations is increased in waveguides with larger period, a to keep the effective slab thickness constant. (b) Dispersion diagrams for the fundamental TE modes of the corrugated waveguides shown in (a). The dispersion diagram of the corrugated waveguide with $a = 32$ and $r = 11$ calculation cells (analyzed in Figure 5) is also shown for comparison.

modes are mainly confined in the middle slab of the PBG waveguide. Therefore, their properties can be modified by changing the geometry of only the air holes that are adjacent to the middle slab.

We also presented here a systematic way of designing dielectric-core photonic crystal waveguides with only one mode in the photonic bandgap. We showed that by increasing the radii of the air holes that are adjacent to the middle slab, we can push the higher order mode(s) out of the photonic bandgap. Our results suggest that more control on the properties of the guided modes can be obtained by changing both the sizes and the period of the air columns adjacent to the middle slab.

Finally, we showed that the properties of the confined modes of a PBG waveguide can be calculated with good accuracy by replacing it with an effective corrugated waveguide that represents only the structure in the vicinity of the middle slab. Replacing a PBG waveguide with its equivalent corrugated waveguide is an effective tool for understanding and designing PBG waveguides. It reduces the computation time of the structures considerably. It enables us to derive approximate analytic formulas for the important properties of the PBG waveguides. Such formulas are usually the best starting points in optimizing the structures. Fine tuning of the optimization can then be performed by full numerical simulation of the actual PBG waveguide.

ACKNOWLEDGMENTS

Partial support of this research was provided by the Woodrow W. Everett, Jr. SCEEE Development Fund in cooperation with the Southeastern Association of Electrical Engineering Department Heads.

REFERENCES

1. E. Yablonovitch, "Inhibited spontaneous emission in solid state physics and electronics," *Phys. Rev. Lett.* **58**, pp. 2059-2062, 1987.
2. S. John, "Strong localization of photons in certain disordered dielectric superlattices," *Phys. Rev. Lett.* **58**, pp. 2486-2489, 1987.
3. P. Yeh and A. Yariv, "Bragg reflection waveguides," *Opt. Commun.* **19**, pp. 427-430, 1976.
4. A. Mekis, J. C. Chen, I. Kurland, S. Fan, P. R. Villeneuve, and J. D. Joannopoulos, "High transmission through sharp bends in photonic crystal waveguides," *Phys. Rev. Lett.* **77**, pp. 3787-3790, 1996.

5. S. Lin, E. Chow, V. Hietala, P. R. Villeneuve, and J. D. Joannopoulos, "Experimental demonstration of guiding and bending electromagnetic waves in a photonic crystal," *Science* **282**, pp. 274–276, 1998.
6. T. Baba, N. Fukaya, and J. Yonekura, "Observation of light propagation in photonic crystal optical waveguides with bends," *Electronic Letters* **35**, pp. 654–655, 1999.
7. M. Tokushima, H. Kosaka, A. Tomita, and H. Yamada, "Lightwave propagation through a 120 degrees sharply bent single-line-defect photonic crystal waveguide," *Appl Phys Lett* **76**, pp. 952–954, 2000.
8. N. Stefanou and A. Modinos, "Impurity bands in photonic insulators," *Phys Rev B* **57**, pp. 12127–12133, 1998.
9. A. Yariv, Y. Xu, R. K. Lee, and A. Scherer, "Coupled-resonator optical waveguide: a proposal and analysis," *Opt. Lett* **24**, pp. 711–713, 1999.
10. M. D. B. Charlton, G. J. Parker, and M. E. Zoorob, "Recent developments in the design and fabrication of visible photonic band gap waveguide devices," *J. Mater. Sci.-Mater. El.* **10**, pp. 429–440, 1999.
11. I. El-Kady, M. M. Sigalas, R. Biswas, and K. M. Ho, "Dielectric waveguides in two-dimensional photonic bandgap materials," *J. Lightwave Technol.* **17**, pp. 2042–2049, 1999.
12. A. Chutinan and S. Noda, "Highly confined waveguides and waveguide bends in three-dimensional photonic crystal," *Appli. Phys. Lett.* **75**, pp. 3739–3741, 1999.
13. V. N. Astratov, D. M. Whittaker, I. S. Culshaw, R. M. Stevenson, M. S. Skolnick, T. F. Krauss, and R. M. D. L. Rue, "Photonic band-structure effects in the reflectivity of periodically patterned waveguides," *Phys. Rev. B* **60**, pp. R16255–R16258, 1999.
14. H. Benisty, D. Labilloy, C. Weisbuch, C. J. M. Smith, T. F. Krauss, D. Cassagne, A. Beraud, and C. Jouanin, "Radiation losses of waveguide-based two-dimensional photonic crystals: Positive role of the substrate," *Appl. Phys. Lett.* **76**, pp. 532–534, 2000.
15. S. Kuchinsky, D. C. Allan, N. F. Borrelli, and J. C. Cotteverte, "3d localization in a channel waveguide in a photonic crystal with 2d periodicity," *Opt. Commun.* **175**, pp. 147–152, 2000.
16. A. Adibi, Y. Xu, R. K. Lee, A. Yariv, and A. Scherer, "Properties of slab modes in photonic crystal optical waveguides," *J. Lightwave Technol.* **18**, pp. 1554–1564, 2000.
17. A. Adibi, Y. Xu, R. K. Lee, A. Yariv, and A. Scherer, "Guiding mechanisms in dielectric-core photonic crystal optical waveguides," *Phys. Rev. B* **64**, pp. 033308 (1–4), 2001.
18. K. S. Yee, "Numerical solution of initial boundary value problems involving maxwell's equations in isotropic media," *IEEE Trans. Antennas Propag.* **AP-14**, pp. 302–307, 1966.
19. C. T. Chan, Q. L. Yu, and K. M. Ho, "Order-n spectral method for electromagnetic-waves," *Phys Rev B* **51**, pp. 16635–16642, 1995.
20. J. P. Berenger, "A perfectly matched layer for the absorption of electromagnetic waves," *J. Comput. Phys.* **114**, pp. 185–200, 1994.
21. Y. Xu, J. S. Vuckovic, R. K. Lee, O. J. Painter, A. Scherer, and A. Yariv, "Finite-difference time-domain calculation of spontaneous emission lifetime in a microcavity," *J. Opt. Soc. Am. B* **16**, pp. 465–474, 1999.
22. Y. Xu, R. K. Lee, and A. Yariv, "Propagation and second-harmonic generation of electromagnetic waves in a coupled-resonator optical waveguide," *J. Opt. Soc. Am. B* **17**, pp. 387–400, 2000.
23. A. Adibi, Y. Xu, R. K. Lee, M. Loncar, A. Yariv, and A. Scherer, "Role of distributed bragg reflection in photonic crystal optical waveguides," *Phys. Rev. B* **64**, pp. 041102(1–4), 2001.
24. A. Yariv, *Optical Electronics in Modern Communications*, Oxford University Press (New York, New York), 1996.
25. A. Adibi, R. K. Lee, Y. Xu, A. Yariv, and A. Scherer, "Design of photonic crystal optical waveguides with single-mode propagation in the photonic bandgap," *Electron. Lett.* **36**, pp. 1376–1378, 2000.